International Journal of Soft Computing 10 (1): 25-36, 2015
ISSN: 1816-9503

Classification of Interstitial Lung Diseases Using Particle Swarm Optimized Support Vector Machine

[1]Anita Titus, [1]H. Khanna Nehemiah and [2]A. Kannan
[1]Ramanujan Computing Centre, Anna University,
[2]Department of Information Science and Technology, Anna University,
Chennai-600025, Tamilnadu, India

Abstract: A Computer Aided Diagnosis (CAD) System for the detection of Interstitial Lung Diseases (ILDs) like emphysema, ground glass opacity, fibrosis and micro nodules based on the texture analysis of lung Computed Tomography (CT) slices has been proposed. The texture features are extracted from the lung region using the Gray Level Histogram (GLH). Quincunx Wavelet Transform (QWT) is applied to the lung regions and the distribution of the wavelet coefficients is modeled using the Gaussian Mixture Model (GSM) of two Gaussians with fixed mean and variable standard deviations. The standard deviations of the two Gaussians are estimated using the Expectation-Maximization (EM) algorithm. The feature vectors constructed from the texture features extracted using the GLH and the QWT are applied to the Support Vector Machine (SVM) classifier. The SVM classifier is optimized using particle swarm optimization and is used to classify the different lung tissue patterns. The classifier achieved an overall precision of 90.23%, accuracy of 96.01% and misclassification rate of 3.99%.

Key words: Interstitial lung diseases, particle swarm optimization, support vector machine, gray level histogram, Computer Aided Diagnosis (CAD)

INTRODUCTION

Interstitial Lung Diseases (ILDs) also referred to as diffuse infiltrative lung diseases are a broad heterogeneous group of diseases that affect the interstitium leading to respiratory failure if the cause of the disease is not identified and treated. There are over 100 diseases that come under the ILD group and only a subset of these diseases like emphysema, ground glass opacity, fibrosis and micro nodules has been considered in this research. The lungs infected with ILDs exhibit different pathological tissue patterns that include consolidations, Ground Glass Opacities (GGO), reticular patterns, reticulonodular opacities, micro nodules, tree in bud patterns, cysts, cavities and honeycombing. As the disease progresses, it affects the shape and size of the lung parenchyma. In rare cases a patient with ILD may have the clinical symptoms but can have a normal radiograph or CT. In such cases, the clinicians base their findings on the medical history of the patient, clinical context and the radiological findings as reported by Ryu *et al*. (2007) and Raghu and Brown (2004).

Computer Aided Diagnosis (CAD) is one of the areas of major research in the field of medical imaging and radiology. The output of a CAD System can be used mainly by non specialist radiologists along with other clinical and laboratory results to obtain a second opinion before making a diagnosis but it does not replace them state by Doi (2007) and Stoitsis *et al*. (2006). A CAD system extracts the texture features from the CT slices and then classifies them. Some of the processes that are applied to the CT slices in this research are discussed as:

The Gaussian Mixture Model and Expectation Maximization algorithm: A simple Gaussian Mixture Model (GMM) consists of a linear superposition of two Gaussians that will be capable of characterizing the image dataset in a better manner than a simple Gaussian distribution. A sufficient number of Gaussians can be used and their means and covariances can be varied so that the dataset is properly characterized. The Expectation Maximization (EM) algorithm proposed by Dempster *et al*. (1977) can be used to find the maximum likelihood solutions and is applied to the Gaussian Mixture Model (GMM).

Support vector machine classifier and particle swarm optimization: The Support Vector Machine (SVM) was introduced by Boser *et al*. (1992). Lee *et al*. (2009) stated that it was one among the best classifiers. The SVM is a

Corresponding Author: H. Khanna Nehemiah, Ramanujan Computing Centre, Anna University, Chennai-600025 Tamilnadu, India

classification tool that uses machine learning to improve its predictive accuracy. The SVM was initially developed to solve the classification problem. Particle Swarm Optimization (PSO) is a stochastic optimization technique introduced by Kennedy and Eberhart (1995), inspired by the social behavior of bird flocking, fish schooling and general swarming behavior. PSO is a Population-Based Search Method that exploits the concept of social sharing of information. Here, an individual or particle's social behavior is influenzed by the behavior of the swarm. This means that each individual (called particle) of a given population (called swarm) can benefit from the previous experiences of all other individuals in the same population. The social behavior is modeled as a multi dimensional space that is collision free in which each particle (candidate solution) will adjust its flying velocity and position according to its own flying experience as well as those of the other companion particles in the swarm.

In this research, a CAD System is proposed for classifying lung texture patterns corresponding to emphysema, GGO, fibrosis, micro nodules and healthy. The main contribution of this research is in optimizing the feature extraction and classification schemes using PSO to improve the classification results.

Literature review: Korfiatis *et al.* (2010) in their research have proposed a CAD scheme for identifying and quantifying Interstitial Pneumonia (IP) patterns in multidetector CT (MDCT) datasets. A 3D Histogram Thresholding algorithm was combined with an edge-highlighting wavelet preprocessing step. The vessel tree structure was segmented next by applying a 3D multiscale filter to enhance the vessels. Then, the EM algorithm was used to threshold the voxels. The vessel tree regions were removed from the lung fields to obtain the lung parenchyma. The Gray-Level Co-occurrence Matrix (GLCM) was calculated from 13 GLCM-based features were extracted. The dimensions of the feature vectors formed were reduced using Stepwise Discriminant Analysis (SDA) and the reduced feature vectors were applied to the K-Nearest Neighbor (KNN) classifier.

Lee *et al.* (2009) in their research have analyzed the performance of several machine classifiers that were used to differentiate obstructive lung diseases in HRCT images. Initially automatic lung segmentation was performed. The blood vessels and the chest wall were removed by thresholding. After segmenting the lung, different sizes of Region of Interest (ROIs) were considered and texture analysis was performed. Four descriptors were used in this research and each ROI was represented using a 13-dimensional feature vector. Naive Bayesian, Bayesian, Artificial Neural Network (ANN) and SVM classifiers were compared experimentally based on the training time, testing time, accuracy, sensitivity and specificity. The SVM classifier outperformed all the other classifiers as it was reasonably fast in training and its sensitivity and specificity were small.

Depeursinge *et al.* (2012) in their research have proposed a near-affine-invariant set of texture features based on wavelet transform to discriminate between healthy and diseased HRCT lung images. The images were of the size 512×512. The ROIs were sub-divided into 32×32 blocks. Healthy tissue was annotated from the normal portions of the diseased lungs. Semiautomatic segmentation based on region growing and mathematical morphological operations were used to obtain the lung regions. The seed point for the region growing process was defined by the user and each 26-connected neighbor was added to the region. The resulting image contained holes which were filled using closing morphological operations. Next each 2D slice was divided into overlapping blocks of size 32×32. For each block the Gray Level Histogram (GLH) was applied with 22 bins and the number of air pixels in each block was also computed, resulting in a single 23-dimensional feature vector. The Quincunx Wavelet Frame (QWF) coefficients were also computed for each block which were then concatenated with the GLH feature vector. Each feature was then normalized by mapping between 0 and 1. The normalized features were applied to a one versus one SVM classifier to differentiate between five classes of lung tissue types namely normal, emphysema, GGO, fibrosis and micro nodules.

Elizabeth *et al.* (2012) have proposed a CAD system for selecting a significant slice from a set of slices of a CT scan to analyze the nodules that correspond to lung cancer. A set of chest CT images, each consisting of multiple slices were selected. Each slice was initially thresholded using Otsu's algorithm. Canny operator was used to detect the edges of the binary image. Morphological and connectivity operations were carried out on the edge detected image to obtain the thresholded lung. A greedy snake algorithm was then applied to reconstruct the lung borders and get the segmented lung parenchyma. The tumour regions were extracted by using a region growing approach and all regions that were non-candidate nodules were removed using a morphological erosion filter. The regions that were not present at the same location in the previous and next slice were pruned and regions that were not pruned constituted the ROIs. The shape and texture features of the ROIs were extracted to form the feature vectors. The feature vectors were used to train a Radial Basis Function Neural Network (RBF NN). ROIs that were >9 pixels and that

existed in atleast three consecutive slices were considered as nodules. The slice containing the ROIs with the largest area was selected as the significant slice.

Darmanayagam *et al.* (2013) in their research have developed a CAD System to detect bronchiectasis, TB and pneumonia using a novel segmentation approach to segment lung parenchyma from the chest CT images with severe pathology attached to the borders. The chest CT image was first denoised using an adaptive Wiener Filter. The edges of the image were then extracted using Laplacean filters. The lung parenchyma was extracted from the rest of the chest CT images by iterative thresholding and morphological fill and close operations used to remove the background, airways and the non-lung components. The shape features were extracted from the segmented lung and given as input to the trained feed forward back propagation Neural Network (NN). The output of the neural network consisted of two classes: completely segmented lung and incompletely segmented lung. Next the ROIs were extracted using region growing algorithm and shape and texture features were extracted. The GLCM was created for each ROI and features were extracted from it. A back propagation NN was trained with the features and an inference subsystem was used to generate the diagnostic results. An accuracy of 97.37%, specificity of 97.71% and precision of 95.74% were obtained by the system.

Comparing with the existing researches discussed in literature, the research discussed in this study is different in the following aspects: PSO is used to optimize the order of the QWF γ and the number of decomposition levels N of the QWF. The number of decomposition levels and the order of the QWF together determine the number of wavelet coefficients that are extracted. Hence, PSO has been used in this research to select the best subset of optimal discriminative features from the set of features derived from the QWF after applying GMM with EM algorithm. The effectiveness of the wavelet coefficients in improving the classification accuracy is enhanced in this research by optimizing γ and N for the classification task using PSO. The best values of cost C and kernel parameter σ of the SVM classifier are also optimized as these parameters influence the effectiveness of the classifier. The research has been tested on real time lung CT slices collected from scan centers in Chennai.

MATERIALS AND METHODS

The flowchart of the proposed CAD System is described in the following sequence: segmentation, feature extraction and classification with wavelet parameters optimization. Figure 1 depicts the overall block diagram. Each process in the system is described in the following study:

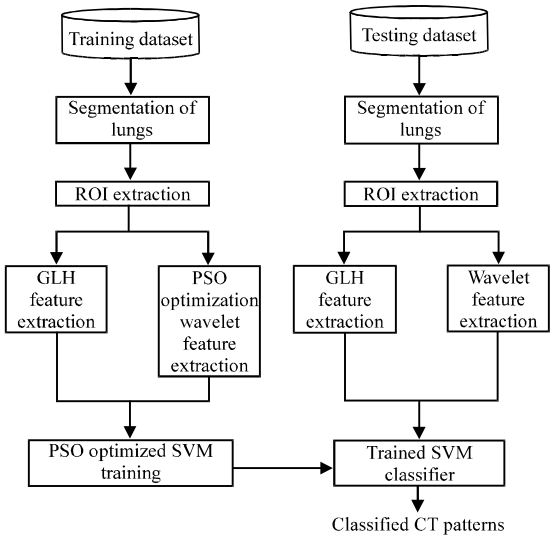

Fig. 1: Block diagram of the proposed CAD System

Segmentation: The segmentation process isolates the lung parenchyma from the surrounding structures in the slice which decreases the volume of the data to be analyzed. The CT slices in JPEG format of size 512×512 pixels are taken as the input. The images are next converted to grayscale for segmentation. The processes involved in segmentation are: optimal thresholding, extraction of lung regions, elimination of small connected components, edge detection and closing mathematical morphology operations.

Optimal thresholding: Optimal thresholding is the initial preprocessing step in segmenting the lung CT slice that consists of high-intensity body pixels and low-intensity pixels that are in the lung and the surrounding air. Optimal thresholding selects a threshold automatically for each CT image based on the variations in the intensity levels. An initial threshold value T is computed that groups the pixels in the 2D slice into two groups G_1 and G_2. Let the mean value of the pixels in G_1 be μ_a and the mean value of the pixels in G_2 be μ_b. The mean value of μ_a and μ_b is computed as the new threshold value T_i using Eq. 1 as given by Hu *et al.* (2001):

$$T_i = \frac{1}{2}(\mu_a + \mu_b) \quad (1)$$

The next new threshold is calculated based on the average values of the pixels in both the groups. The process of computing the new threshold continues iteratively until the difference between consecutive threshold values is 0.1.

Input: Chest CT Scan grayscale image.

Process logic

Step 1: The histogram of the grayscale slice is computed.

Step 2: Compute the initial threshold value. The ratio of the sum of all the intensity levels in the slice to the total number of pixels is the mean intensity value of the slice. This is the initial threshold value.

Step 3: This threshold separates the pixels into two groups. The first group of pixels has intensity values that are greater than or equal to the threshold. The second group of pixels has intensity values lesser than the threshold.

Step 4: The average intensity values are computed for both the groups of pixels and a new threshold is determined by computing the mean of these two values.

Step 5: From the newly computed threshold, the steps 3 and 4 are repeated until the thresholds obtained in successive iterations remains a constant.

Step 6: Pixels whose intensity values are greater than the threshold value are converted to white and pixels with intensity values lesser than or equal to the threshold are converted to black.

Output: Thresholded binary chest CT slice.

Lung region extraction: The region growing algorithm is one of the simplest Region-Based Segmentation Methods used to segment an image by initially selecting a set of points, known as seed points. This technique groups pixels that are spatially close as those pixels will have similar intensity and texture values. A seed point is chosen and all pixels that are the 8-neighbors of the seed point are first added to the region, if they satisfy the threshold conditions. Pixels are constantly added to the region surrounding the seed point, if they satisfy the required criterion and if they are connected to the pixels in the region by 8-connectivity. The region keeps growing until no further pixels satisfy the intensity and connectivity conditions.

Input: Thresholded binary chest CT slice (Output of optimal thresholding process).

Process logic

Step 1: The thresholded CT slice is complemented.

Step 2: The seed point for the region is selected by determining a pixel whose intensity value is lesser than the optimal threshold value that was determined by the optimal thresholding process.

Step 3: A pixel is added to the seed point if the difference between a pixel's intensity value and the region's mean is the smallest difference and if the pixel being considered is a four neighbor of the seed pixel.

Step 4: The region grows iteratively by assigning all unallocated neighboring pixels to the region.

Step 5: Region growing stops when the intensity difference between region mean and the candidate pixel being considered exceeds the threshold condition.

Output: Binary CT slice without the background pixels.

Elimination of the airways and edge detection: The trachea and airways are non lung components that must be separated from the lungs. So, the connectivity of the thresholded image from the previous step is computed to determine the total number of connected regions. All the connected components in the image are labeled so that all the pixels in a connected region have the same label. The number of labels depends on the number of connected components in the image. The number of pixels in each connected component is determined from its region properties. In the experimental setup the airways are connected components with an area that varies between 500 and 600 pixels. This value is determined based on the trials conducted on several scans and on the resolution of the CT slice since as the resolution of the CT slice changes, the number of pixels per inch will also vary. Hence, all components with areas between 500 and 600 pixels are eliminated. The edges of the lungs are then detected using the Sobel edge detector.

Input: Binary CT slice without the background pixels (Output of the removal of background pixels process).

Process logic

Step 1: The total number of connected components in the binary CT slice is computed based on the 8-connectivity of neighboring pixels. The pixels of each connected component are then labeled.

Step 2: The areas of the connected components are determined and all components whose area is between 500 and 800 pixels are filled with zeros by using a morphological open operation. This eliminates the trachea and any other small connected components that are present outside the lungs.

Step 3: The edges of the lungs are next detected using the Sobel edge detector.

Output: Edge detected binary image in which the airways have been eliminated.

Extraction of the Region of Interest (ROI): The edge detected image contains holes that are not connected to the border of the image. So, they are not eliminated when the border pixels are cleared. Therefore, the holes are filled using a morphological fill operation. If the pathological regions in the image are at the periphery of the lungs then the shape of the lung border gets changed. The lung borders are reconstructed using the convex hull morphological operations.

Input: Edge detected output image (Output of removal of airways and edge detection process).

Process logic

Step 1: All the regions outside the lung are set to zero as the disease is not located outside the lung.

Step 2: Holes that are present inside the lung regions are filled.

Step 3: Convex hull operator is applied to the image to reconstruct and obtain the complex shape of the lung border.

Step 4: Each white pixel present in the region is replaced by its original grayscale value and all black pixels are left unchanged resulting in a segmented grayscale image containing the right and left lungs.

Step 5: Next partition the segmented image into 32×32 blocks.

Step 6: All sub-blocks that consist of only black pixels and the sub-blocks that contains <75% of the lung region are discarded. The remaining sub-blocks are the Regions of Interest (ROIs).

Output: Extracted ROIs.

Feature extraction: The feature extraction technique applied in this proposed research was proposed by Depeursinge *et al.* (2012). The features are extracted from the ROIs using the Gray Level Histogram (GLH) and Quincunx Wavelet Frame (QWF) decomposition followed by GMM with EM algorithm.

Gray level histogram: The Gray Level Histogram (GLH) characterizes the distribution of the gray levels in the image. It gives an estimate of how many pixels possess a particular gray level intensity value which corresponds to the density of the lung tissue. The GLH characterizes the global feature composition of an image and it is invariant to translation and rotation of the images (Park *et al.*, 2000). The distribution of the gray level values in the histograms shows high variations for the five types of lung tissue patterns. To extract texture information from the ROIs, GLHs with 22 bins are constructed as given by Eq. 2 for each ROI:

$$H = \{bin_0, bin_1, ..., bin_{21}, pix_{air}\} \quad (2)$$

where, $\{bin_0, bin_1, ...bin_{21}\}$ represents 22 histogram bins and pix_{air} represents the number of pixels in the ROI with grayscale value '0' corresponding to black which is computed as an additional feature. To determine the grayscale intensity values in the [0-255] display range based on the Hounsfield Units (HU), Eq. 3 as given by Horwood *et al.* (2001) is used:

$$y\ (grayscale) = 127.5+0.1275x \quad (3)$$

here, when x = -1000 then y = 0 and when x = 600 then y = 204

Input: Extracted ROIs (Output of extraction of ROIs process).

Process logic

Step 1: In each ROI determine the minimum and maximum HUs using Eq. 3 when x = -1000 and x = 600.

Step 2: Initialize the number of histogram bins to 22.

Step 3: Calculate the bin width using Eq. 4 to determine the bin positions starting from the minimum value and extending to the maximum value:

$$Binwidth = \frac{Max\ value-(Min\ value+1)}{Number\ of\ bins} \quad (4)$$

Step 4: Compute the number of pixels in each bin. These values form the GLH features.

Step 5: Plot the histogram of all the ROIs for pixel values ranging from 0-255 for the values computed in step 4.

Step 6: For each ROI, the number of pixels in the 22 histogram bins $\{bin_0, bin_1, ..., bin_{21}\}$ and the number of pixels with intensity value 0 $\{pix_{air}\}$ are concatenated to form the GLH feature vector of the ROI.

Output: 23 GLH features for each ROI.

Quincunx Wavelet Frame (QWF) decomposition: Wavelets are a family of mathematical functions that are obtained by repeatedly translating and dilating a mother wavelet. It decomposes the image into elementary forms at different positions and scales and assigns a frequency range to each scale component (where the scale is the inverse of the frequency). This results in a set of wavelet coefficients N_c corresponding to the different scales and to the different frequency directions. These wavelet coefficients N_c are proportional to the number of pixels in the input image N_{pixels} the number of iterations J and the number of sub-bands per iteration $N_{subband}$ and is represented by Eq. 5:

$$N_c = N_{pixels} \times J \times N_{subband} \quad (5)$$

The texture parameters can be computed from the wavelet coefficients.

Input: Extracted ROIs (output of extraction of ROIs process).

Process logic

Step: Compute the wavelet coefficients by applying QWF decomposition using the optimal parameters γ (order) and N (number of decomposition levels).

Output: Wavelet coefficients for each sub-band.

Gaussian Mixture Model (GMM) with Expectation Maximization (EM) algorithm: The GMM is used to compute the texture parameters from the wavelet coefficients. The distributions of the wavelet coefficients in each sub band are characterized by the parameters of a simple GMM of two Gaussians. A GMM with two Gaussians is selected having mean values μ_1 and μ_2 and standard deviations σ_1 and σ_2. The initial values of μ_1, μ_2, σ_1 and σ_2 are first chosen. Following this the EM algorithm is applied. The EM algorithm consists of two steps: the Expectation (E) step and the Maximization (M) step. The E step takes the current values of the parameters to evaluate the conditional probabilities of class membership. The probabilities obtained in the E step are then used to re-estimate the mean values in the M step. The new values of the means are then used to re-compute the standard deviation values in the M step. The parameters are updated in the E step followed by the M step until the algorithm converges. The updated mean μ and standard deviation σ values are estimated using the EM algorithm. The E and M step together form one iteration.

Input: Wavelet coefficients for each sub band (output of QWF decomposition).

Process logic

Step 1: The two Gaussians are assigned a weight of 0.5 each as proposed by Depeursinge *et al.* (2012). The mean values of the two Gaussians μ_1, μ_2 are kept a constant such that $\mu_1 = \mu_2 = \mu$. The mean value of the wavelet coefficients in each sub band is S_j using which the mean value μ of the GMM is initialized.

Step 2: The standard deviations σ_1 and σ_2 are initialized using Eq. 6 from the range r_{Sj} of the wavelet coefficients. The range of the wavelet coefficients is given by Eq. 6 where:

$$r_{S_j} = \max(S_j) - \min(S_j) \quad (6)$$

Then:

$$\sigma_1 = r_{S_j}, \ \sigma_2 = \frac{r_{S_j}}{10}$$

Step 3 (Expectation step): The values are classified into one of the two Gaussian mixtures using Eq. 7:

$$C_j = P_j \frac{1}{\sigma\sqrt{2\pi}} e^{-\frac{1}{2}\left(\frac{x-\mu}{\sigma}\right)^2} \quad (7)$$

Where:

P_j = The probability of each class
j = The total number of classes ranging from 1 to N
σ = The standard deviation of each class
μ = The mean of the wavelet coefficients
x = A random variable
C_j = The data of each class

Step 3 (Maximization step): Estimate the parameter σ of each class as given by Eq. 8:

$$\sigma_i = \sqrt{\frac{\sum C_j \left(x-\mu_j\right)^2}{\sum C_j}} \quad (8)$$

Step 4: Steps 2 and 3 are iterated until convergence.

Output: Three GMM parameters are computed.

The feature vector v is next computed by concatenating the 23 GLH features and the three GMM features calculated for eight iterations from 0-7 as given by Eq. 9:

$$v = \begin{Bmatrix} bin_0, bin_1, ..., bin_{21}, pix_{air}, \mu^0, \sigma_1^0, \sigma_2^0, \\ \mu^1, \sigma_1^1, \sigma_1^2, ..., \mu^7, \sigma_1^7, \sigma_2^7 \end{Bmatrix} \quad (9)$$

Each feature vector that is extracted is normalized by mapping between 0 and 1 to achieve scale invariance. The normalized feature vectors of the images are given as input to the SVM classifier.

Multiclass texture classification with particle swarm optimization: The SVM classifier with a Gaussian kernel learns from the space spanned by the feature vector v to find the decision boundaries among five classes of lung tissue types using a one-versus-all approach. This system is designed to optimize the order of the quincunx wavelet γ and the number of decompositions N. The PSO does a velocity update and a position update of the particles. The velocity with which each particle gets accelerated in the search space changes during each iteration and the new velocity of the particle depends on the current velocity, the distance between the previous best position and the previous global best position. The next position of the particle depends on the particle's new velocity. Each iteration of the PSO algorithm has three steps which are repeated until a stopping criterion is satisfied. First the fitness of each particle is evaluated. Next the individual best and global best fitness values and position values are updated. Finally, the velocity and position of each particle is computed. The optimization process is illustrated in Fig. 2.

Input: QWF parameters (N, γ) and SVM parameters (c, σ).

Process logic

Step 1: Initialize a swarm of particles with N, γ, c and σ data.

Step 2: Initialize the maximum number of iterations and decide the stopping criterion: maximum number of iterations (MAX_ITER =).

Step 3: Set the acceleration constants, inertia weight and random constants for each particle (c_1 and c_2 are acceleration constants that are set to 2.0; ω(t) is the inertia weight set to 0.729 and r_1, r_2 are random values in the range [0, 1] based on Eberhart and Shi (2001).

Step 4: Initialize the velocity vectors v_i associated with the particles.

Step 5: Train the SVM with selected PSO selected QWF features and SVM parameters.

Step 6: Compute the fitness of each particle P_i based on Eq. 10 and 11:

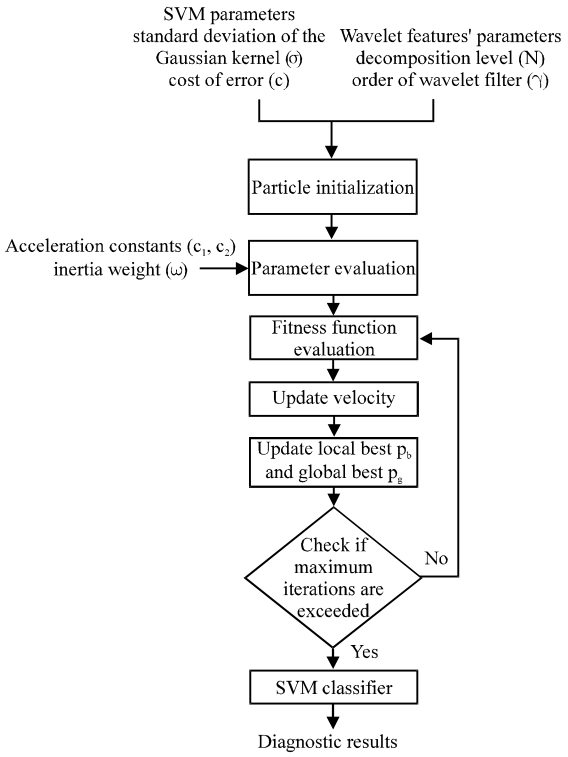

Fig. 2: Block diagram of PSO process

$$Fitness(P_i) = Accuracy(P_i) \quad (10)$$

where, P_i is a set of inputs to the SVM:

$$Accuracy(P_i) = \frac{TP+TN}{TP+TN+FP+FN} \quad (11)$$

Step 7: Update the velocity of each particle using Eq. 12:

$$v_i(t) = w(t)v_i(t-1) + c_1r_1(p_b(t)-x_i(t-1)) + c_2r_2(p_g(t)-x_i(t-1)) \quad (12)$$

Where:

- t = Current time and (t-1) is the previous time step
- w(t) = Inertia weight
- $v_i(t)$ = Current velocity of particle i
- c_1 and c_2 = Acceleration constants that are positive and usually set to 2.0
- r_1 and r_2 = Positive random values taken from a uniform distribution in the range [0, 1]
- p_g = Local position the particle
- p_b = Best of particle i
- x_i = Position global best position of the particle
- i = Total number of particles

Step 8: Update the current position of each particle by adding its velocity using Eq. 13:

$$x_i(t) = x_i(t-1)+v_i(t) \quad (13)$$

Step 9: Repeat steps 5-8 till stopping criterion is reached.

Output: SVM classifier.

RESULTS AND DISCUSSION

This research distinguishes normal from pathological CT scans (emphysema, fibrosis, GGO and micro nodules) by studying their textural parameters. The dataset of lung CT scans consists of 20 normal scans, 26 scans with micro nodules, 21 scans with emphysema, 14 scans with fibrosis that exhibited honeycombing and 21 scans with GGO as listed in Table 1.

By analyzing the texture features of these scans, the system distinguishes between the different classes of the CT slices. The lung CT slice was first segmented using the Region Growing algorithm to obtain the lung parenchyma. The segmented lung was then sub-divided into 32×32 blocks and blocks that had >75% of the lung parenchyma were alone considered for further processing. The GLH was used to extract 23 histogram features from each sub block which were normalized and fed to the SVM.

Table 1: Images tested

Type of CT image	Total scans	Total slices	Training ROIs	Testing ROIs
Healthy	20	50	558	335
Emphysema	21	50	457	274
GGO	21	50	382	229
Micro nodules	26	50	345	207
Fibrosis	14	50	435	261
Total	102	250	2177	1306

The different stages of the segmentation process for a fibrosis CT slice are illustrated in Fig. 3. The segmented lung images are next divided into 32×32 blocks. Blocks which have >75% of the lung regions are selected and these constitute the ROIs while all other blocks are eliminated. Texture features are extracted from the ROIs.

Determination of GLH features: Grayscale values contain valuable information for the characterization of objects and textures. GLHs show variability of their distributions among the patterns. The histograms of the ROIs are illustrated in Fig. 4. The GLH is constructed by dividing the grayscale range of 0-255 into 22 bins and the distribution of pixels in each bin is computed. The pixels corresponding to gray level zero corresponding to air pixels is also computed. So, overall 23 texture features are computed from the GLH. The computed features are then normalized between 0 and 1.

Determination of wavelet transform features: Wavelet transform is applied to the ROIs to extract the texture features. For the classification of lung tissue patterns, a subset of features able to characterize the coefficients of the wavelet filter banks is required. The wavelet frame transform yields a number of wavelet coefficients for each sub band. From these coefficients, the texture parameters (μ, σ_1, σ_2) for each sub band are computed. The features derived from the Quincunx wavelet transform depends on

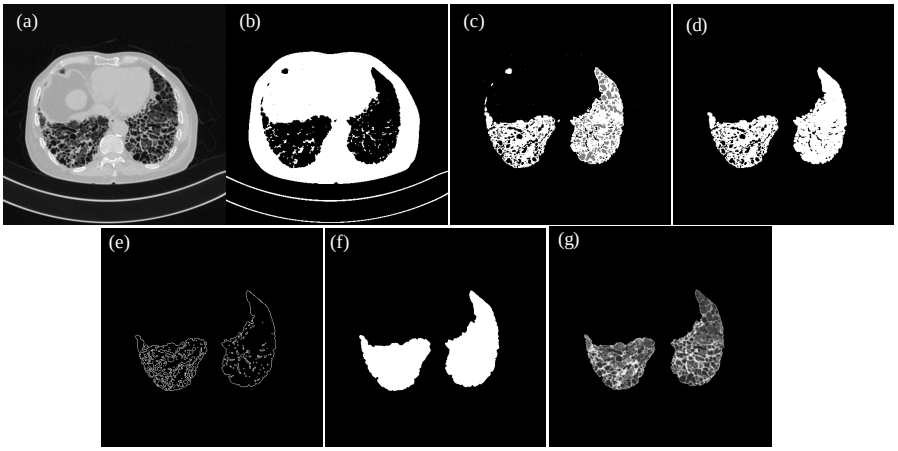

Fig. 3: Segmentation results of a fibrosis image; a) input image; b) thresholded image; c) output of region growing stage; d) elimination of small connected components; e) edge detected image; f) holes filled image and g) segmented image

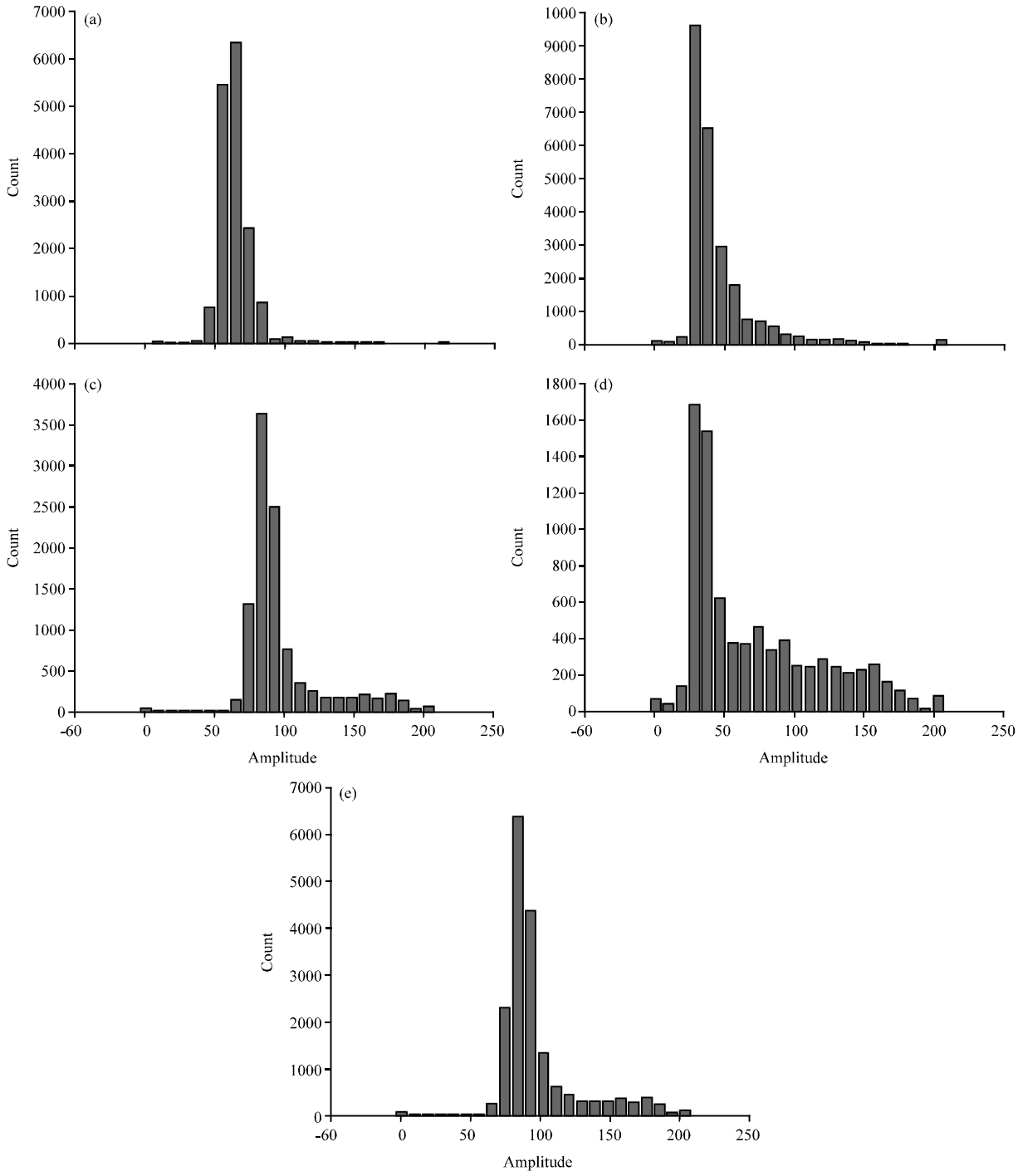

Fig. 4: Gray level histogram of lung tissue patterns; a) healthy; b) emphysema; c) GGO; d) fibrosis and e) micro nodules

the number of decomposition levels. Figure 5 illustrates the QWF coefficients of sub bands from normal and pathological lung tissue patterns for a single ROI. PSO is used to find optimal wavelet parameters (gamma and number of decomposition levels).

Classification results: True Positive (TP) refers to all the blocks that have been correctly classified as diseased by the CAD system and have also been diagnosed by the radiologist as diseased. True Negative (TN) refers to all the blocks that have been classified by both the CAD

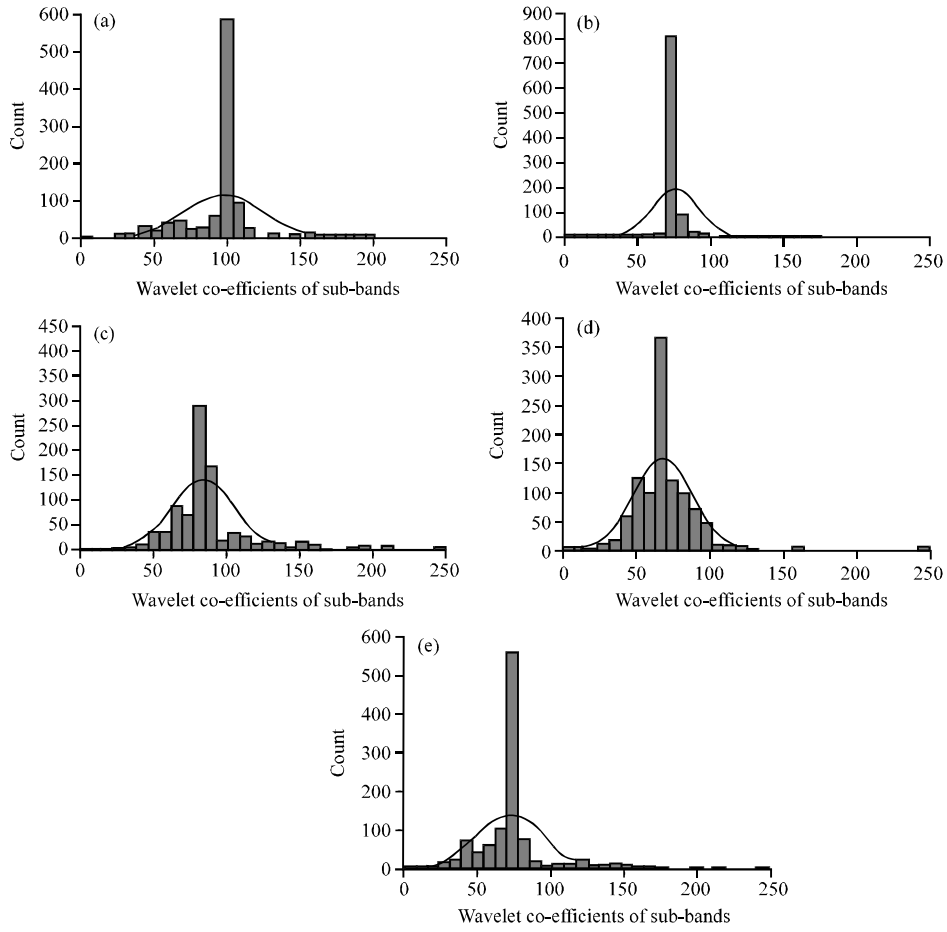

Fig. 5: Quincunx wavelet frame values of sub-bands; a) normal; b) emphysema; c) ground glass; d) fibrosis and e) micro nodules

System and the radiologist as normal. False Negative (FN) refers to all the blocks that have been classified as normal by the CAD System but have been diagnosed as diseased by the radiologist. False Positive (FP) refers to all blocks that have been classified as diseased by the CAD System but have been diagnosed as normal by the radiologist. Sensitivity and specificity describe as to how well the classifier discriminates between cases with positive class and with negative class (with and without disease). Sensitivity is the proportion of cases with positive class that are classified as positive (true positive rate, expressed as a percentage). Specificity is the proportion of cases with the negative class, classified as negative (true negative rate, expressed as a percentage). Various performance measures of the system such as specificity, accuracy, precision and recall for both SVM without PSO and for SVM with PSO based optimized wavelet parameters are calculated using the Eq. 11 and 14-23:

$$\text{Specificity or True Negative Rate (TNR)} = \frac{TN}{TN+FP} \quad (14)$$

$$\text{Recall or sensitivity or True Positive Rate (TPR)} = \frac{TP}{TP+FN} \quad (15)$$

$$\text{Precicion or Posititive Predictive Value (PPV)} = \frac{TP}{TP+FP} \quad (16)$$

$$\text{Native Predictive Value (NPV)} = \frac{TN}{TN+FN} \quad (17)$$

$$\text{False Positive Rate (FPR)} = 1\text{-Specificity} = \frac{FP}{TN+FP} \quad (18)$$

$$\text{False Negative Rate } (FNR) = 1 - \text{Sensitivity} = \frac{FN}{TP+FN} \quad (19)$$

Table 2: Classification results without PSO

	CT image				
Metric	Healthy	Emphysema	GGO	Micro nodules	Fibrosis
Specificity	94.93	93.72	94.26	96.72	96.64
Sensitivity	87.80	77.80	83.90	76.20	82.20
Accuracy	93.06	90.25	92.36	93.29	93.60
Precision	85.96	77.50	76.74	82.32	86.72
Negative Predictive Value (NPV)	95.64	93.81	96.29	95.30	95.32
False Positive Rate (FPR)	5.07	6.28	5.74	3.28	3.36
False Negative Rate (FNR)	12.24	22.22	16.10	23.83	17.78
False Discovery Rate (FDR)	14.04	22.50	23.26	17.68	13.80
Positive Likelihood Ratio (PLR)	17.32	12.38	14.63	23.24	24.47
Negative Likelihood Ratio (NLR)	0.13	0.24	0.17	0.25	0.18
Misclassification rate	6.94	9.75	7.64	6.71	6.40

Table 3: Classification results with PSO

	CT image				
Metric	Healthy	Emphysema	GGO	Micro nodules	Fibrosis
Specificity	96.52	96.92	97.72	98.33	97.85
Sensitivity	91.64	88.32	89.08	90.29	91.19
Accuracy	95.24	95.09	96.18	97.04	96.49
Precision	90.29	88.64	89.47	91.18	91.54
Negative Predictive Value (NPV)	97.03	96.83	97.63	98.14	97.75
False Positive Rate (FPR)	3.48	3.08	2.28	1.67	2.15
False Negative Rate (FNR)	8.36	11.68	10.29	9.71	8.81
False Discovery Rate (FDR)	9.71	11.36	10.53	8.82	8.46
Positive Likelihood Ratio (PLR)	26.29	28.72	39.09	53.97	42.32
Negative Likelihood Ratio (NLR)	0.09	0.12	0.11	0.09	0.09
Misclassification rate	4.76	4.91	3.82	2.96	3.51

$$\text{False Discovery Rate (FDR)} = 1 - \text{Precision} = \frac{FP}{TP+FP} \quad (20)$$

$$\text{Positive Likelihood Ratio (PLR)} = \frac{TPR}{FPR} \quad (21)$$

$$\text{Negative Likelihood Ratio (NLR)} = \frac{FNR}{TNR} \quad (22)$$

$$\text{Misclassification rate} = \frac{FP+FN}{TP+TN+FP+FN} \quad (23)$$

The performance measures of the CAD System are computed in Table 2 and 3. Table 2 shows the results obtained for classification without parameter optimization. The proposed PSO-SVM Classification System aims at enhancing the SVM classification process in two different ways: tuning of the value of the two wavelet parameters along with SVM parameters and detecting the best set of discriminative features since the number of features derived from the QWF depends on the number of decomposition levels. Table 3 shows the results obtained for classification with parameter optimization using PSO.

From this experimental research, it is observed from Table 2 that though the SVM performs well for the default wavelet parameters, its accuracy and misclassification rate can still be improved by optimizing its wavelet parameters. Table 3 shows that the use of PSO based optimization frame research for classifying lung textures yielded significant improvement in the performance of the system.

CONCLUSION

In this research, a particle swarm optimized SVM has been used in the design of a CAD System for classifying the lung tissue patterns from Computed Tomography (CT) images of patients affected with Interstitial Lung Diseases (ILDs). Five lung tissue patterns (normal, emphysema, GGO, fibrosis and micro nodules) are classified using a SVM classifier that was optimized using PSO from the features extracted using GLH and QWF. The system has achieved an average specificity of 97.47%, precision of 90.23% and recall of 90.1%. The average misclassification rate is 3.994. The results show that the use of the PSO based optimization frameresearch for classifying lung CT patterns resulted in significant improvement and allowed an average accuracy of 96.01% of correct matches among the 5 lung tissue classes of the test sets. An area to be addressed is that when an image that does not belong to any of these classes is applied, the system classifies the query image into whichever class that closely matches it. So, this proposed research can be further extended to consider the effect of adding lung CT images corresponding to other ILDs and also to quantify the diseased regions and determine the severity of the ILD in CT lung images.

REFERENCES

Boser, B.E., I.M. Guyon and V.N. Vapnik, 1992. A training algorithm for optimal margin classifiers. Proceedings of the 5th Annual Workshop on Computational Learning Theory, July 27-29, 1992, Pittsburgh, Pennsylvania, USA., pp: 144-152.

Darmanayagam, S.E., K.N. Harichandran, S.R.R. Cyril and K. Arputharaj, 2013. A novel supervised approach for segmentation of lung parenchyma from chest CT for computer-aided diagnosis. J. Digit. Imag., 26: 496-509.

Dempster, A.P., N.M. Laird and D.B. Rubin, 1977. Maximum likelihood from incomplete data via the EM algorithm. J. R. Stat. Soc., 39: 1-38.

Depeursinge, A., D. Van de Ville, A. Platon, A. Geissbuhler, P.A. Poletti and H. Muller, 2012. Near-affine-invariant texture learning for lung tissue analysis using isotropic wavelet frames. IEEE Trans. Inform. Technol. Biomed., 16: 665-675.

Doi, K., 2007. Computer-aided diagnosis in medical imaging: Historical review, current status and future potential. Comput. Med. Imag. Graph., 31: 198-211.

Eberhart, R.C. and Y. Shi, 2001. Particle swarm optimization: Developments, applications and resources. Proceedings of the Congress on Evolutionary Computation, Volume 1, May 27-30, 2001, Seoul, South Korea, pp: 81-86.

Elizabeth, D.S., H.K. Nehemiah, R. Raj and A. Kannan, 2012. Computer-aided diagnosis of lung cancer based on analysis of the significant slice of chest computed tomography image. IET Image Processing, 6: 697-705.

Horwood, A.C., S.J. Hogan, P.R. Goddard, J. Rossiter, S.H. Ma and P.G. Bsc, 2001. Image normalization, a basic requirement for computer-based automatic diagnostic applications. http://facweb.cs.depaul.edu/research/vc/seminar/Paper/Feb22_2008Emili_ImageNormalization.pdf.

Hu, S., E.A. Hoffman and J.M. Reinhardt, 2001. Automatic lung segmentation for accurate quantization of volumetric X-ray CT images. IEEE Trans. Med. Imaging, 20: 490-498.

Kennedy, J. and R. Eberhart, 1995. Particle swarm optimization. Proceedings of the International Conference on Neural Networks, Volume 4, November 27-December 1, 1995, Perth, WA., USA., pp: 1942-1948.

Korfiatis, P.D., A.N. Karahaliou, A.D. Kazantzi, C. Kalogeropoulou and L.I. Costaridou, 2010. Texture-based identification and characterization of interstitial pneumonia patterns in lung multidetector CT. IEEE Trans. Inform. Technol. Biomed., 14: 675-680.

Lee, Y., J.B. Seo, J.G. Lee, S.S. Kim, N. Kim and S.H. Kang, 2009. Performance testing of several classifiers for differentiating obstructive lung diseases based on texture analysis at high-resolution computerized tomography (HRCT). Comput. Methods Programs Biomed., 93: 206-215.

Park, D.K., Y.S. Jeon and C.S. Won, 2000. Efficient use of local edge histogram descriptor. Proceedings of the ACM Workshops on Multimedia, October 30-November 3, 2000, Los Angeles, CA., USA., pp: 51-54.

Raghu, G. and K.K. Brown, 2004. Interstitial lung disease: Clinical evaluation and keys to an accurate diagnosis. Clin. Chest Med., 25: 409-419.

Ryu, J.H., C.E. Daniels, T.E. Hartman and E.S. Yi, 2007. Diagnosis of interstitial lung diseases. Mayo Clin. Proceed., 82: 976-986.

Stoitsis, J., I. Valavanis, S.G. Mougiakakou, S. Golemati, A. Nikita and K.S. Nikita, 2006. Computer aided diagnosis based on medical image processing and artificial intelligence methods. Nuclear Instruments Methods Phys. Res. A, 569: 591-595.